A Numerical Simulation of Meshes Mending Used in the Three-dimensional Porthole Die Extrusion of Thin Wall Profiles

Shao-Yi Hsia[1*]

[1]*Department of Mechanical and Automation Engineering, Kao-Yuan University, Kaohsiung City, 821, Taiwan.*

Author's contribution

Author SYH managed the conceptualisation, methodology, software, formal analysis. Author SYH performed the writing of original draft preparation, review and editing, supervision and project administration.

Original Research Article

ABSTRACT

Aims: The variety of aluminium products used in many industries (e.g., aviation, railroad, and transport) drive the need for an urgent increase in aluminium feedstock. Improved aluminium extrusion forming and mold design guarantee product quality, shorten production time, and enhance mold life. We analyse and discuss the problems resulting from the simulation and analysis of thin-layer aluminium alloy rims by focusing on porthole die extrusion for bicycles. In general, when analysing with CAE, the billet going from portholes to the welding chamber in the hot extrusion forming process indicates that mesh penetration during remesh causes volume loss and stops the simulation. This is especially serious on thin wall products.
Methodology: In this study, applying mesh mending to extrusion of the billet could solve this problem, and the previous issue of mesh contact causing volume disappearance would not appear during simulation. After solving the remesh problem, the optimisation method in the Taguchi Method could be utilised to modify the hot extrusion mold and analyse its existing speed to avoid uneven forming.

Corresponding author: Email: syhsia@cc.kyu.edu.tw;

Results: Our analysis simultaneously examined stress, strain, velocity gradient, and product formation to understand the relationships between parameters and extrusion load as well as forming defects caused by thin wall extrusion. It is expected to provide a specifically practicable analysis model for aluminium extrusion.
Conclusion: Comparing the simulation size with design size ensures accuracy. The maximum size error was 8.70% at a size of 0.92mm, and the maximum error of the rest of the sizes was about ±5%, which was acceptable in this study.

1. INTRODUCTION

Aluminium extrusion is a mature process technology; however, product deformation and bending readily occur in the high-strength aluminium alloy extrusion process, thus failing to achieve customer required standards. This situation is even more serious with thin-walled materials.

Chanda et al. applied 3D Finite Element Analysis software, DEFORM-3D, to discuss the effects of extrusion ratio and extrusion speed on the temperature change of Al6061 in the extrusion process [1]. Al6061 was assessed in the 3D Finite Element Analysis with rigid viscoplasticity in the simulation and parameters were established to avoid extrusion defects.

Using the Finite Element Method to simulate extrusion problems, Chanda et al. discovered that if extrusion pressure were lowered by extruding at stepped extrusion speeds, blank and mold temperature would not increase in the extrusion process and pressure distribution caused by extrusion could be reduced [2].

Kim et al. pointed out that welding pressure in the welding chamber is the most important factor in extrusion strength [3]. To enhance welding strength, bridge design is required for the mold. An increase in the angle of inclination allows the blank to flow smoothly through the welding chamber and effect complete welding. By comparing hole expansion testing results of the molds before and after modification, the modified mold had a stronger extrusion welding pressure.

Jo et al. studied the extrusion of window molding with a seam tube through Finite Element Analysis and, focusing on the mold welding cavity, discussed seam tube joint strength and the internal pressure of the welding cavity [4]. The welding pressure of hot extrusion was confirmed through finite element simulation and experiments that analysed metal flow and predicted welding pressure. Finite element simulation and experimental results compared different billet temperatures, bearing lengths, and product thicknesses. These results can be applied to the future design of porthole dies.

Di first used rigid-viscoplastic Finite Element software DEFORM-3D to acquire the effects of die welding chamber depth and bearing length on the physical fields of extrusion pressure, stress & strain, and die stress to further optimise small-diameter thin-walled aluminium pipe through the porthole die extrusion [5]. The simulation presented that upper porthole die stress was mainly distributed in the porthole bridging and mandrel while a lower die stress was focused on the bearing and knuckle area of the welding chamber, and that welding chamber depth and bearing length had great effect on product quality. The test revealed that increasing the welding chamber depth and bearing length enhanced the weld seam strength and surface quality of the products.

He studied metal flow in different directions and pressure distribution in the welding chamber in the 6063 aluminium alloy hollow extrusion process [6]. He also analysed the factors causing defects, and proposed a die repair method; *i.e.*, increasing flow blockers. The simulated result displayed changing velocities in different directions after increasing the flow blockers; especially, internal metal flow obviously decreased to reduce concavity. Comparing the simulation with actual extrusion, it was found that increasing flow blockers produced qualified products. It proved that the Finite Element Method could be used in optimisation research on hot extrusion dies in the complicated extrusion process, which presented certain reference values for the actual production process.

To analyse the uneven flow in aluminium extrusion, Li et al. utilised DEFORM-3D Finite Element Analysis software for analysing metal

flow when extruding 6005A aluminium alloy square pipe through a three-hole dual-core die [7]. The simulation showed that uneven porthole area distribution could easily result in defects of the sickle curvature on the square pipe. When the ratio of the middle porthole and side porthole areas was 0.93～1.03, exit flow was even and the weld seam was in the middle.

Huang et al. applied developed remesh techniques for the welding process to analyse the effects of welding chamber depth and welding angle on forming quality when analysing square pipe porthole die double-hole extrusion [8]. Their results revealed that the average hydrostatic pressure on the welding surface, effective stress at the bottom of the porthole bridging, and maximum core offset increased with increasing welding chamber depth.

Zhang et al. established the geometric model of a plane porthole die with UG NX [9]. This research also used Finite Element software DEFORM-3D in the extrusion process to study metal flow in aluminium alloy hollow extrusion. The simulation revealed that even the conventionally designed well-symmetric aluminium alloy window die (with a symmetric axis) did not avoid uneven metal flow affecting the degree of forming.

Gagliardi et al. using a Taguchi method based on a special design of orthogonal array with the grey relational analysis [10]. The influences of the investigated geometric variables on three extrusion outputs, e.g., the required ram load, the maximum pressure inside the welding chamber, and the material flow homogeneity, were highlighted by ANOVA technique, and the Grey relational analysis was also introduced determining an optimal combination of the investigated parameters.

Liu et al. simulated the design of a porthole die for producing aluminium profiles using HyperXtrude 13.0 software based on ALE formulation [11]. The simulation results indicated a design method for porthole die for aluminium with a high length–width ratio and small cavity, including sunken port bridges to rearrange the welding chamber in upper die, introducing the baffle plate, and adjusting the bearing length.

Ji et al. designed a porthole die based on the theory of metal plastic forming, and established a finite element model of the extrusion process for a hollow aluminium alloy profile [12]. Results

showed that the uneven deformation caused by the difference in wall thickness was the main factor that causes the uneven distribution of grain sizes in the cross-section of the product.

The above research gradually solved some of the problems in the aluminium forming process, but there are many more problems that still require research effort. One of these especially is the mutual penetration of meshes appearing on Finite Element software from the welding chamber to the exit that occurs when aluminium alloy rims are under hot extrusion welding pressure. In order to solve this problem, a mesh mending technology was used in this study. Hence, the porthole die used for aluminium hot extrusion was analysed through Finite Element Analysis software, DEFORM-3D, or the best parameter combination with optimum process was discussed. Extrusion load, effective stress, effective strain, and velocity gradient were acquired with software analysis.

2. FUNDAMENTAL THEORY

2.1 Porthole Extrusion Process

A porthole die is operated by applying a solid billet that is split into several metal flows through portholes under extrusion pressure to gather in a welding chamber under high temperature and high pressure for re-welding, and eventually flow out through the gap between the mandrel and die hole to form the required product. Metal flow in the porthole die is very complex because of the complicated die structure. Fig. 1 shows the hot extrusion process in which the billet Al 6061 (Table 1) from the container through the welding chamber to exit the porthole die and bearing as the ram moves forward.

A porthole die is divided into an upper die and a lower die (Figs. 2 and 3). An upper die contains some portholes, porthole bridging, and a mandrel. The porthole is the channel through which metal flows, porthole bridging supports the mandrel, and the mandrel is used for forming the shape and size of the product cavity. A lower die includes a welding chamber, die hole, and bearing. The welding chamber gathers metal from the porthole and the bearing confirms the external size and shape of the product and regulates metal flow. A dowel pin is used for positioning upper/lower dies, and a connecting screw tightly connects the upper and the lower dies so that the porthole die become a single piece for convenient operation and strength enhancement.

Table 1. Material parameters of Al 6061 used in the simulation

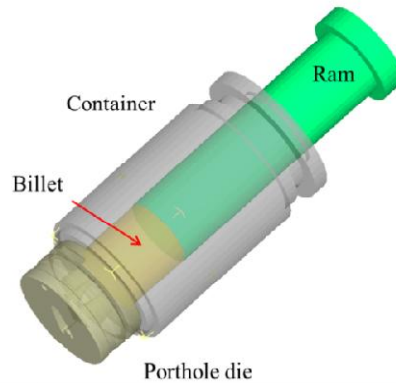| Si	Fe	Cu	Mn	Mg	Cr	Zn	Ti
0.4-0.8	0-0.7	0.15-0.4	0-0.15	0.8-1.2	0.04-0.35	0-0.25	0-0.15

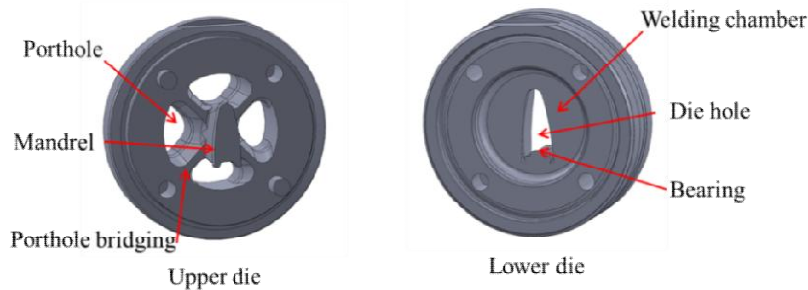**Fig. 1. Transparent three-dimensional model of porthole die**
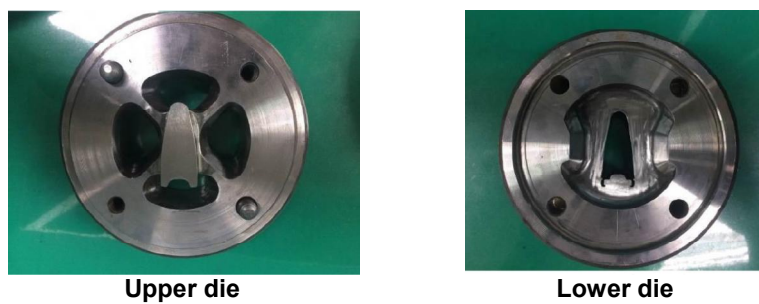

Fig. 2. Structured schematic diagram of porthole die

Fig. 3. Experimental apparatus of porthole die

Fig. 4 shows the different forms of aluminium alloy rims that were used for this simulation. Since the thin wall aluminium rim going from portholes to the welding chamber in the hot extrusion forming process would cause mesh penetration and volume loss during welding, this feature leads to an incorrect simulation when analysing with CAE.

2.2 Forming Theory

2.2.1 True stress and strain

Based on the initial cross-sectional area A_0 and the initial height h_0 of the metal, the stress σ_0 and the strain ε_0 are calculated and the relationship curve is called the engineering stress-strain
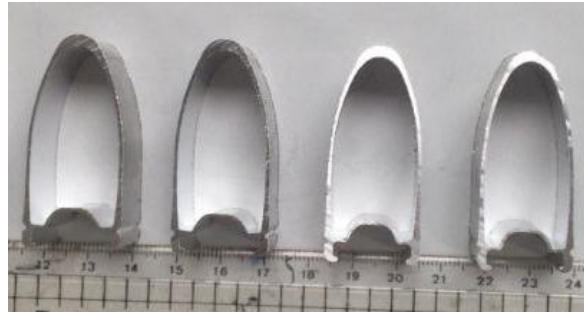
4

Fig. 4. Cross-section photos of different forms of aluminium alloy rim

curve. However, the curve is not the actual stress and strain relationship in that it does not provide real deformation characteristics. To solve this problem, Ludwik first proposed the idea of true stress and true strain, the equation for which is shown below [13].

$$\text{Reduction ratio}: r = \frac{h_0 - h}{h_0} \qquad (1)$$

$$\text{Engineering stress}: \sigma_0 = \frac{p}{A_0} \qquad (2)$$

$$\text{Engineering strain}: \varepsilon_0 = \frac{h_0 - h}{h_0} \qquad (3)$$

$$\text{True stress}: \sigma_t = \sigma_0(1-r) \qquad (4)$$

$$\text{True strain}: \varepsilon_t = \ln(1-r)^{-1} \qquad (5)$$

where h_0 is initial height, h is final height, A_0 is original area, and p is ram load.

2.2.2 Metal yield criteria

Yield criteria refer to the hypotheses of a metal elastic boundary under any possible stress. According to yield criteria, the occurrence of metal plastic deformation under stress can be judged. The accuracy of any suggested yield criteria need to be proven with experiments. The Tresca yield criterion and von Mises yield criterion are commonly utilised in the plastic processing analysis.

(1) The design size based on Tresca theory, which is conservatively secure, is larger than if based on von Mises, which tends to economically secure.
(2) In Tresca theory, only the maximal and the minimal stresses are required, while all major stresses are required for von Mises. The mechanics of materials are generally based on maximal shear stress theory in

Tresca, while machine design refers to the distortion energy theory of von Mises.

2.2.3 Constant shear friction

Friction related to constant shear friction τ_f and shear yield strength k is called constant shear friction, as in the following equation:

$$\tau_f = m \cdot k \qquad (6)$$

where m is the friction factor or shear friction coefficient, and $0 \leq m < 1$. Constant shear friction is applicable to cold/hot/warm forming with larger interfacial pressure. $m = 1.0$ denotes sticking friction and the large hot forge shear stress ($\tau_f = k$ shows the materials are stuck) is generally assumed to be sticking friction.

3. RESEARCH METHODOLOGY

The 3D geometric model of the die in this study was established by scanning a solid porthole die. Fig. 1 shows the transparent three-dimensional chart of the die for successive extrusion processing, including a billet, ram, container, and die. The figure is of a single element that is first transformed into an STL file and then DEFORM-3D forming software is used [14,15]. Fig. 5 is the research flow chart. Aluminium related information was acquired from the literature or the built-in database of the simulation software. The results were compared with the design size of the aluminium alloy rim cross section to evaluate the accuracy of the software or to the referenced analysis parameters.

In this analysis, the die (ram, container, upper die, and lower die) was set to be rigid, the simulated billet set as Al 6061, the heat transfer coefficient set at 20 N/sec/mm/C [16], the constant shear friction factor set at 0.4/0.7 [16], and temperatures set at 450 ℃ for the billet,

about 400 ℃ for the ram and container, and about 480 ℃ for the upper and lower dies.

The parameters used for the simulation were acquired with convergence analysis and the Taguchi Method.

3.1 Convergence

Basically, the Finite Element Method calculation is a numerical iteration. A good iterative method should have the resulting value approach stability with several iterations as iteration differences become progressively smaller. This effect is called convergence in numerical analysis. Contrary to convergence, divergence refers to larger values being produced with increasing numbers of iterations. Convergence is defined in this study as finer grid segmentation resulting in more elements and nodes in the finite element analysis with simulation results having greater accuracy and precision. However, more elements and nodes increase computer computations; *i.e.*, more simulation time being spent. A mesh convergence analysis of the extrusion process in this study, with the same simulation parameters but using mesh numbers 60k, 100k, 150k, and 210k, presents a simulation load of about 797-949kN with a mesh amount of 60k-210k, an error between maximum and minimum values (within 16%), and the aluminium alloy rim at about 100k forming to a certain length at the mold exit. In the beginning of this study, the modeling practicability and stability required a mesh amount of 80k-150k being utilised as the analysis basis.

3.2 Taguchi Method

The Taguchi Method precedes one-time combination with various factors through an orthogonal array to acquire the most information with the least experimental time to rapidly identify optimal parameter conditions. In this section, the characteristics of the Taguchi Method are discussed relative to their effect on various process parameters for billet forming in planning for proper numerical simulation.

3.2.1 Simulation parameter planning

The purpose of optimisation analysis in the Taguchi Method is to lay out the simulation of extrusion forming. An $L_9(3^4)$ orthogonal array is selected in the research process and a total of nine forming analyses are made. Experience indicates that four important control factors are required in the simulation process, namely billet length (mm), size factor of mesh, ram speed (mm/sec), and stoke per step (mm/step). Three levels for each of the above simulation factors plus the control factor design and level of distribution are shown in Table 2. The original aluminium billet height is 80mm, mesh size factor controls the computing scale, ram speed should be adjusted by referring to the process speed in the field, and stoke per step should be smaller than segmented mesh size. The simulation's results of the distribution of the orthogonal array $L_9(3^4)$ are shown in Table 3. Extrusion length in the table refers to the shortest extrusion length from the billet at the mold exit to the end of the simulation that was effective and without deformation. The load is the maximum extrusion force caused by the ram extruding the billet. Extrusion length and extrusion load are not necessarily at the same extrusion stroke. The S/N ratio, which is an indicator of robustness, is the signal/error ratio in the Taguchi Method. Extrusion length is used as the larger-the-better objective function. The extrusion length acquired from this analysis is calculated as the larger-the-better signal-noise ratio, and the optimal simulation parameter combination is revealed by the S/N ratio response table.

3.2.2 S/N ratio factor response table

To match the S/N ratio in Table 3, response Table 4 was acquired with forming length as the larger-the-better objective function. The values of four control factors *A*, *B*, *C*, and D corresponding to Levels 1, 2, and 3 represent the effect of the former on the S/N ratio under the fixed level. Range represents the difference between maximum and minimum values in different levels under the same control factor, with larger values indicating larger effects. Rank is the ordering importance of control factors according to Range, with the effects of the four control factors on quality characteristics being ranked $B > A > D > C$. That is, *B* (size factor of mesh) presents the largest effect on quality characteristics, while *C* (ram speed, mm/sec) appears to have the least influence.

The S/N responses in Table 4 show that the optimal simulation parameter combination is *A*2 *B*3 *C*2 *D*1, meaning that the optimal simulation parameters can be acquired with billet length 80mm, mesh size factor 0.2, ram speed 1.5mm/sec, and stoke per step 0.05mm/step. Simulation parameters herein following refer to Table 5 results.

6

Table 2. Four factors and three levels of the orthogonal array $L_9(3^4)$

Factors	Level 1	Level 2	Level 3
A. Billet length (mm)	50	80	130
B. Size factor of mesh	0.1	0.15	0.2
C. Ram speed (mm/sec)	0.5	1.5	2.5
D. Stoke per step (mm/step)	0.05	0.2	0.3
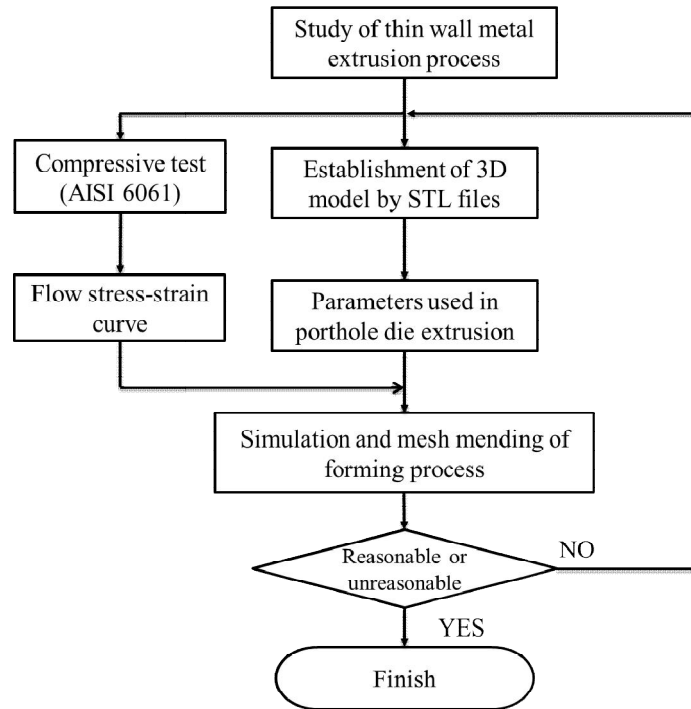
Fig. 5. Research flow chart

Table 3. S/N ratios and extrusion loads using the Taguchi method

No.	Extrusion length (mm)	Extrusion load (kN)	S/N (dB)
1	8.61	760	18.70
2	14.00	890	22.93
3	23.98	996	27.60
4	10.79	1050	20.66
5	16.85	1100	24.53
6	27.77	997	28.87
7	8.03	1140	18.09
8	14.32	801	23.12
9	29.64	1010	29.44

Table 4. Extrusion length response based on S/N ratios

	A	*B*	*C*	*D*
Level 1	23.08	19.15	23.56	24.22
Level 2	24.69	23.52	24.34	23.30
Level 3	23.55	28.64	23.41	23.79
Range	1.61	9.48	0.93	0.93
Rank	2	1	3	3

4. RESULTS AND DISCUSSION

4.1 Welding Stage

The flow of aluminium during hot extrusion can be divided into the three stages of porthole, welding, and forming. After entering the welding chamber, the material mixes as a whole under high temperature and high pressure until the

7

metal is completely welded and flows out from the bearing. In the porthole die extrusion process, the hydrostatic pressure on the welding surface is related to the welding quality of the metal, which directly influences product quality.

Table 5. Software parameter settings

Mesh number	80k~150k
Billet length (mm)	80
Size factor of mesh	0.2
Ram speed (mm/sec)	1.5
Stoke per step (mm/step)	0.05

4.2 Mesh Mending Method

In the DEFORM-3D analysis, the welding stage might not proceed smoothly because of mesh contact. In Fig. 6, the billet starts to be extruded by the ram from the porthole die. At Step 241, the billet passes the porthole and is welded in the welding chamber. Nevertheless, the minimum size of the product at the exit that the meshes would contact during welding to continue the extrusion is merely 0.6mm. This will result in volume disappearance (Fig. 7) during mesh penetration and further affect forming in the welding chamber [17-19]. As a result, the billet cannot be welded in the extrusion process. In this case, applying mesh mending to extrude the billet solves the problem, and volume disappearance will not appear in the simulation process. Fig. 8 shows the mesh mending method of the billet. The process consists of making points on the welding billet in the welding chamber with Nx software, laying out the points

as lines, laying the lines on the front and back surfaces, and laying the surfaces as a solid object to complete the reverse solid file.
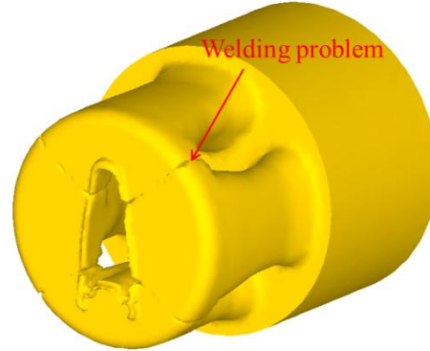

Fig. 6. Position of mesh penetration in billet

Fig. 9 displays the billet at the welding stage and the mending process. The billet from the porthole to the welding chamber is shown in Figs. 9(a) and (b). Fig. 9(c) shows the mesh penetration problem due to the software remesh function, and hence a mesh mending technology (Fig. 9(d)) is necessary to study the thin wall metal extrusion process. Figs. 10 and 11 indicate the effective stress and effective strain distribution of the welding plane in the situation before and after mesh mending. It can be clearly seen that the effective stress and effective strain can always be maintained within a certain range in both cases.
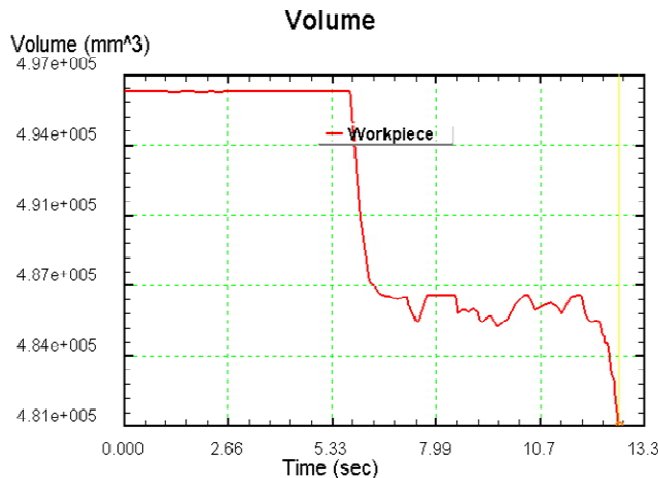

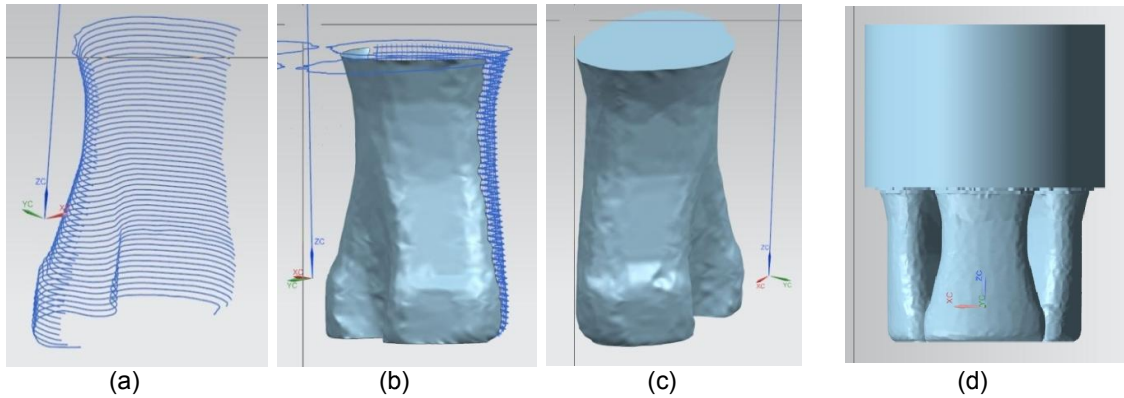**Fig. 7. Volume disappearance caused by billet export forming defects**

Fig. 8. Mesh mending method of billet: (a) laying the points as lines, (b) laying the lines as the surface, (c) laying the surfaces as a solid object, (d) reverse solid file

4.3 Analysis of Extrusion Processes

The billet is extruded from the die exit by a ram. Fig. 12 shows the maximum effective stress (merely 69.19MPa) focuses on the lower part of the container and the direct contact with the upper die after forming the aluminium extruded billet. From Fig. 13, the location of the maximum effective strain (10.61mm/mm) is the same location as that of the maximum effective stress. In Fig. 14, the maximum velocity gradient (98.03mm/sec) appears at the die bearing exit. Fig. 15 indicates the detailed velocity distribution at the exit and the extruded product. The larger velocity occurring above and below the exit

profile will induce an uneven section and curved product. If the final curved aluminium alloy rim isn't desired, some modifications in the porthole die may be considered; for example, a flow promoting block or choke block added in the welding chamber to adjust the flow rate of the extruded billet. The temperature distribution of the billet in the hot extrusion process (Fig. 16) indicates that the temperature increases gradually from the billet to the extruded profile along the extrusion direction. Because the billet in the container is not deformed, its local temperature is lower. Around the welding chamber, the temperature is high (near 500°C) because of severe plastic deformation.
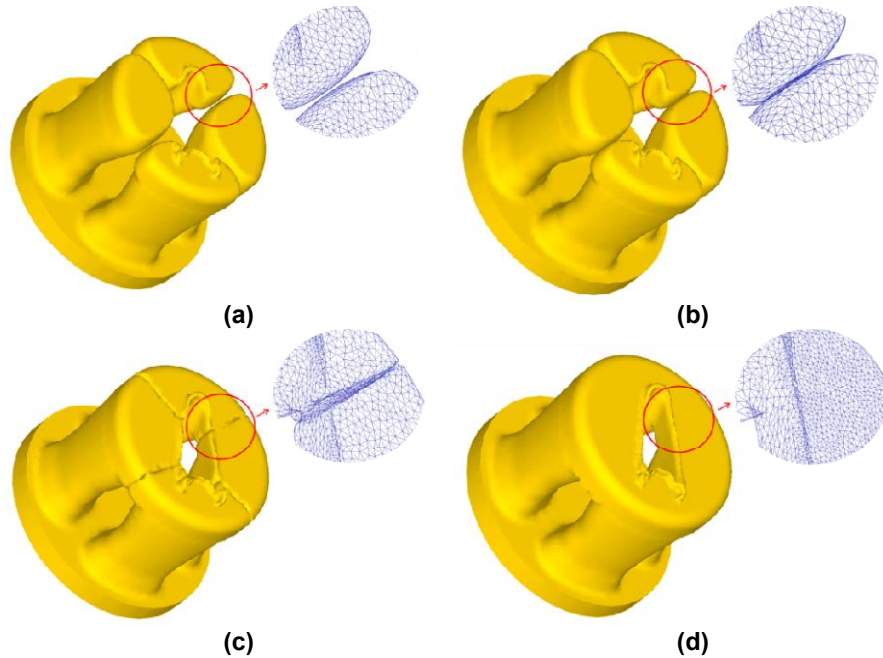

Fig. 9. Extrusion stages and mesh situation of porthole die: (a) diversion, (b) filling and welding, (c) penetration problem, (d) mesh mending
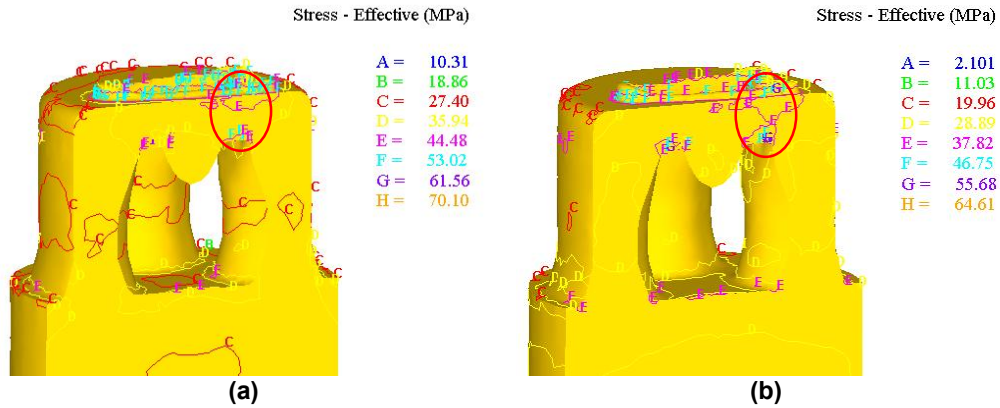
Fig. 10. Effective stress distribution of billet: (a) before mesh mending, (b) after mesh mending
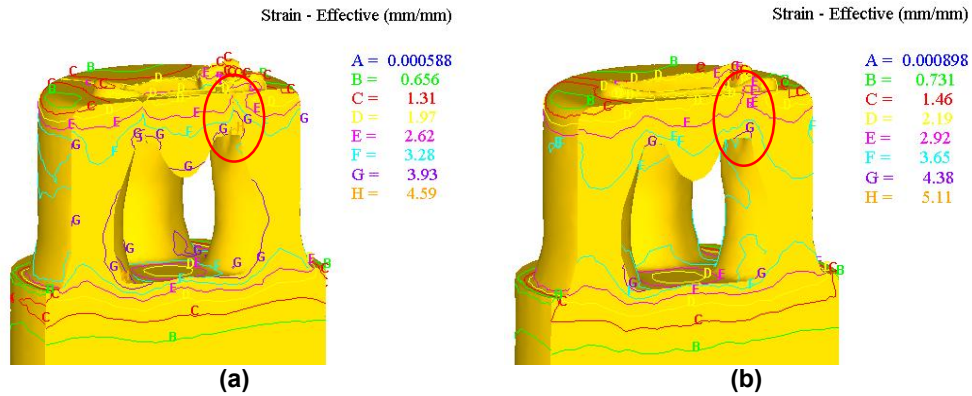

Fig. 11. Effective strain distribution of billet: (a) before mesh mending, (b) after mesh mending
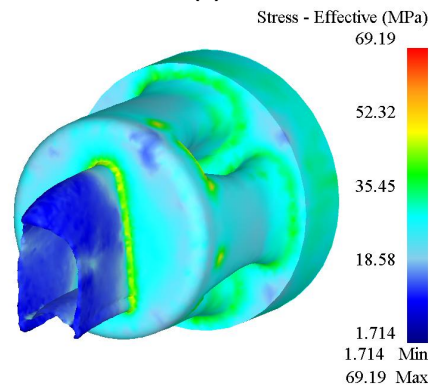

Fig. 12. Effective stress distribution of billet

Fig. 17 shows the distribution of the extrusion load at the three stages of billet extrusion. When the billet is extruded by the ram, extrusion load rapidly increases (*OA* extrusion section). With extrusion of the ram, the billet flows to the porthole of the upper die (AB porthole section) where the extrusion load does not appear to have large differences. After passing through the porthole, the billet passes into the welding chamber and the extrusion force increases as the billet contacts the bottom of the welding chamber (*BC* stage). The forming load reaches its highest value when the billet is extruded by the ram into the welding chamber (*CD* welding and extrusion of material head). After the completion of welding, the billet is

continuously and stably extruded from the exit and formed (*DE),* and the required load is smaller than what is needed during extrusion of the head.
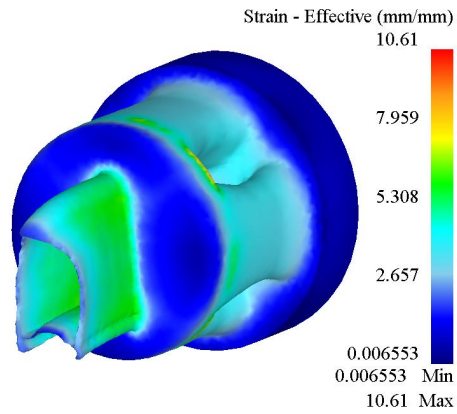

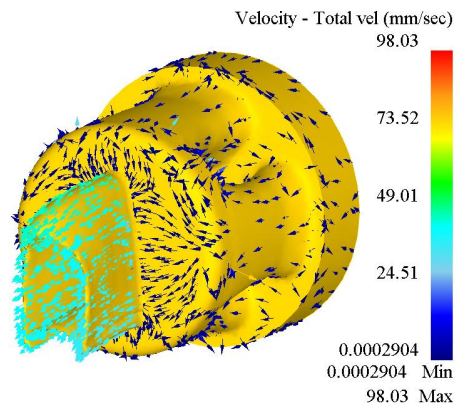
Fig. 13. Effective strain distribution of billet

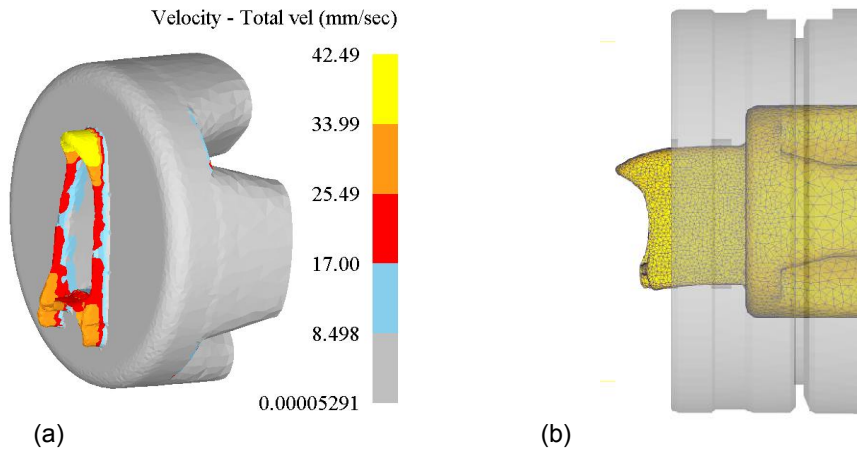**Fig. 14. Velocity gradient distribution of billet**

(a)　　　　　　　　　　　　　(b)

Fig. 15. Velocity gradient distribution of billet and finished product at the exit of the porthole die
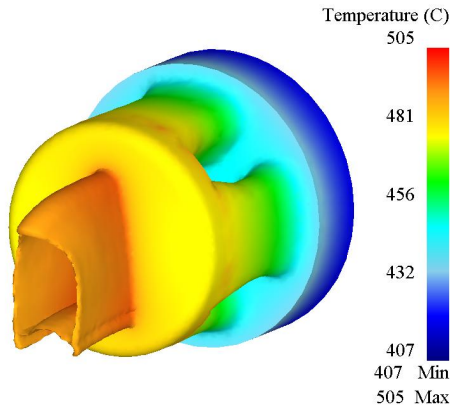
11

Fig. 16. Temperature distribution of billet

Fig. 18 indicates the simulated size and finished aluminium alloy rim product. When comparing the cross sections of the simulated billet and the actual product shown in Fig. 2, the actual physical deformation is demonstrated to have been exactly captured by the simulation. Error sizes are listed in Table 5. The maximum error of 8.70% appeared at 0.92mm, meaning that a smaller cross section of the aluminium alloy rim would result in fewer numbers of meshes distributed. Larger errors appear when describing the forming mechanics of the zone.
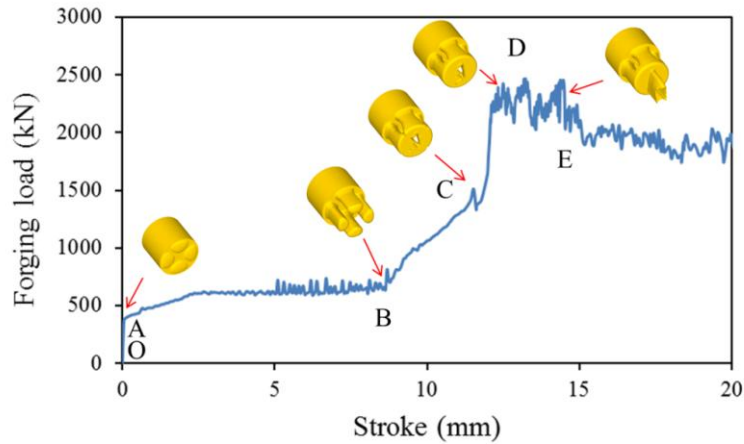

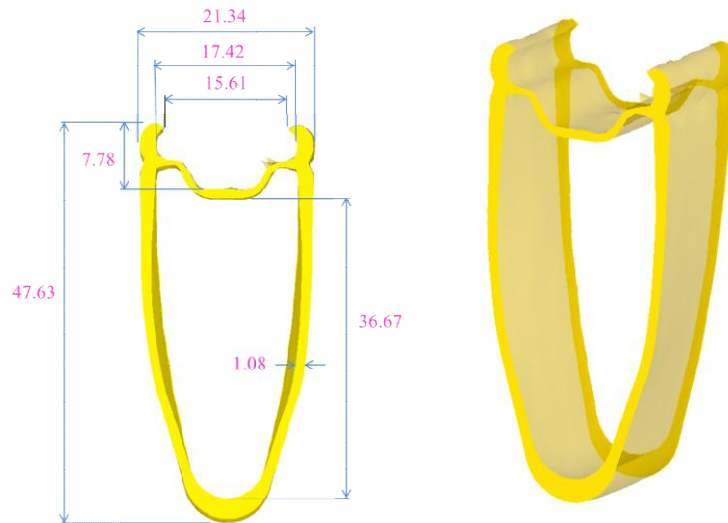**Fig. 17. Forging loads at the different strokes of billet extrusion**

Fig. 18. Simulation size and finished product of the aluminium alloy rim

Table 5. Error comparison between the simulation original die size and designed size of the aluminium alloy rim

Simulation results (mm)	Designed size (mm)	Error (%)
47.63	47.00	1.33
7.78	8.00	-2.71
21.34	20.50	4.10
17.42	17.01	2.43
15.61	15.00	4.06
36.67	36.30	1.01
1.00	0.92	8.70

4. CONCLUSION

DEFORM-3D was utilised in this study for analysing simulations of hot extrusion. Comparisons to the solid die are:

(1) In the forming process analysis, mesh mending was able to overcome the problem of billet penetration into the welding chamber. The mended billet was proven to successfully extrude during the forming simulation.
(2) The maximum effective stress during forming was focused on the area where the container bottom directly contacts the upper die and the maximum velocity gradient appeared on the die bearing exit.
(3) Comparing simulation size and design size ensures accuracy. The maximum size error was 8.70%, which appeared at a size of 0.92mm, and the maximum error of the rest of the sizes was about ±5%, which was acceptable in this study.

This study combined CAD and CAE to provide a simulation of the aluminium alloy rim extrusion process for use by forming businesses. It could reduce the costs of manpower and production as well as savings on materials consumption and the reduction of equipment loss.

ACKNOWLEDGEMENTS

COMPETING INTERESTS

Author has declared that no competing interests exist.

REFERENCES

1. Chanda T, Zhou J, Kowalski L, Duszczyk J. 3D FEM simulation of the thermal events during AA6061 aluminum extrusion. Scripta Materialia. 1999;41(2):195-202.
2. Chanda T, Zhou J, Duszczyk J. A comparative study on iso-speed extrusion and isothermal extrusion of 6061 Al alloy using 3D FEM simulation. Journal of Materials Processing Technology. 2001; 114(2):145-153.
3. Kim KJ, Lee CH, Yang DY. Investigation into the improvement of welding strength in three-dimensional extrusion of tubes using porthole dies. Journal of Materials Processing Technology. 2002;130:426-431.
4. Jo HH, Jeong CS, Lee SK, Kim BM. Determination of welding pressure in the non-steady-state porthole die extrusion of improved Al7003 hollow section tubes. Journal of Materials Processing Technology. 2003;139(1-3):428-433.
5. Di LQ, Zhang SH. Numerical Simulation of Extrusion Process and Design of Mold Optimization. Journal of Plasticity Engineering. 2009;162:123-127.
6. He X. Numerical simulation of extrusion process of hollow profile and optimization of mold structure. Thesis of Master Degree. Hunan University; 2010.
7. Li JY, Huang DN. Analysis of extrusion flow behaviors of square pipe deformed with three-porthole and two-core die. Materials Science and Technology. 2010;18(2):251-255.
8. Huang DN, Zhang ZH, Li JY, Xie JX. Influences of welding chamber depth and welding angle on forming quality of extrusion of square tube by porthole die. The Chinese Journal of Nonferrous Metals. 2010;205:954-960.
9. Zhang Y, Deng XM. Finite Element simulation and die optimization design of aluminum extrusion process. Nonferrous Metal Processing. 2010;39(3):36-39.
10. Gagliardi F, Ciancio C, Ambrogio G. Optimization of porthole die extrusion by Grey-Taguchi relational analysis. Int. J. Adv. Manuf. Tech. 2018;94:719–728.
11. Liu Z, Li L, Li S, Yi J, Wang G. Simulation Analysis of Porthole Die Extrusion Process and Die Structure Modifications for an Aluminum Profile with High Length–Width Ratio and Small Cavity. Materials. 2018;11:1517.

12. Ji H, Nie H, Chen W. Ruan X, Pan P, Zhang J. Optimization of the extrusion die and microstructure analysis for a hollow aluminum alloy profile. Int. J. Adv. Manuf. Tech. 2017;93:3461–3471.

13. Altan T, Ngaile G, Shen G. Cold and Hot Forging: Fundamentals and Applications. 1st ed.; ASM International: Geauga, OH, USA. 2005;295–298.

14. Hsia SY, Shih PY. Wear improvement of tools in the cold forging process for long hex flange nuts. Materials. 2015;8:6640–6657.
DOI:10.3390/ma8105328.

15. Hsia SY, Chou YT, Lu GF. Analysis of Sheet Metal Tapping Screw Fabrication Using a Finite Element Method. Applied Sciences. 2016;6:300.
DOI:10.3390/app6100300.

16. Youfeng H, Shuisheng X, Jun X, Lei C, Guoji H. Numerical simulation on extrusion process of aluminum profile with large and complex cross-section and die structure optimization. Materials Research and Application. 2011; 5(3):203-208.

17. Jo HH, Lee SK, Jung CS, Kim BM. A non-steady state FE analysis of Al tubes hot extrusion by a porthole die. Journal of Materials Processing Technology. 2006; 173:223–231.

18. Li L, Zhang H, Zhou J, Duszczyk J, Li GY, Zhong ZH. Numerical and experimental study on the extrusion through a porthole die to produce a hollow magnesium profile with longitudinal weld seams. Materials and Design. 2008;29:1190–1198.

19. Liu G, Zhou J, Duszczyk J. FE analysis of metal flow and weld seam formation in a porthole die during the extrusion of a magnesium alloy into a square tube and the effect of ram speed on weld strength. Journal of Materials Processing Technology. 2008;200:185–198.